

# Results from a Future Linear Collider Energy Spectrometer Prototype

A. Lyapin<sup>a</sup>, H.J. Schreiber<sup>b</sup>, M. Viti<sup>b</sup>, C. Adolphsen<sup>c</sup>, R. Arnold<sup>c</sup>,  
S. Boogert<sup>d</sup>, G. Boorman<sup>d</sup>, F. Gournaris<sup>a</sup>, V. Duginov<sup>e</sup>, C. Hast<sup>c</sup>,  
M. Hildreth<sup>g</sup>, C. Hlaing<sup>h</sup>, F. Jackson<sup>i</sup>, O. Khainovsky<sup>h</sup>, Y. Kolomensky<sup>h</sup>,  
S. Kostromin<sup>e</sup>, B. Maiheu<sup>a</sup>, D. McCormick<sup>c</sup>, D. J. Miller<sup>a</sup>, N. Morozov<sup>e</sup>,  
T. Orimoto<sup>h,j</sup>, M. Slater<sup>f</sup>, Z. Szalata<sup>c</sup>, M. Thomson<sup>f</sup>, D. Ward<sup>f</sup>, M. Wing<sup>a</sup>,  
M. Woods<sup>c</sup>

<sup>a</sup>University College London, London, UK

<sup>b</sup>Deutsches Elektronen Synchrotron DESY Hamburg and Zeuthen, Germany

<sup>c</sup>SLAC National Accelerator Laboratory, Menlo Park, California, USA

<sup>d</sup>Royal Holloway, University of London, Egham, UK

<sup>e</sup>Joint Institute for Nuclear Research, Dubna, Moscow Region, Russia

<sup>f</sup>University of Cambridge, Cambridge, UK

<sup>g</sup>University of Notre Dame, Notre Dame, Indiana, USA

<sup>h</sup>University of California and Lawrence Berkeley National Laboratory, Berkeley,  
California, USA

<sup>i</sup>Daresbury Laboratory, Daresbury, UK

<sup>j</sup>California Institute of Technology, Pasadena, California, USA

---

## Abstract

The International Linear Collider and other proposed high energy  $e^+e^-$  machines aim to measure the Standard Model quantities and new, not yet discovered phenomena with unprecedented precision. One of the main requirements for achieving this goal is a measurement of the incident beam energy with an uncertainty of  $10^{-4}$  or less. This article describes the performance of a prototype energy spectrometer commissioned in 2006-2007 in SLAC's End Station A beamline. The prototype was a 4-magnet chicane equipped with several beam position monitors restoring the beam orbit through the chicane. An energy resolution close to  $5 \cdot 10^{-4}$  was estimated, which, however, needs to be improved for use in a linear collider. We also report on the operational experience with the prototype and devise ways of improving the performance of the chicane-based spectrometer.

*Keywords:* Energy measurement, Energy Spectrometer, Cavity Beam

---

<sup>1</sup>This work was supported by the Commission of the European Communities under the 6th Framework Programme "Structuring the European Research Arm," contract number RIDS-011899 and by the Science and Technology Facilities Council (STFC)

<sup>2</sup>This work was supported by the U.S. Department of Energy under contract DE-AC02-76SF00515

<sup>3</sup>This work was supported by the U.S. Department of Energy under contract DE-FG02-03ER41279

## 36 1. Introduction

37 The physics potential of the next TeV-energy Linear Collider depends  
38 greatly on precision energy measurements of the electron and positron beams  
39 at the interaction point (IP). Such measurements are mandatory in order to  
40 determine particle masses in high-rate processes. For example, measuring  
41 the top mass from a threshold scan to order of 100 MeV or measuring the  
42 Standard Model Higgs in direct reconstruction to about 50 MeV requires  
43 knowledge of the luminosity-weighted mean collision energy to a level of  $1 -$   
44  $2 \cdot 10^{-4}$  to avoid center-of-mass energy ( $\sqrt{s}$ ) uncertainties from dominating  
45 the experimental results. Incoming beam energy ( $E_b$ ) measurements are a  
46 critical component to  $\sqrt{s}$  determination as it sets the overall energy scale for  
47 the collision process.

48 The strategy proposed in the International Linear Collider (ILC) design  
49 [1] is to have redundant beam-based measurements capable to achieve a  $10^{-4}$   
50 relative precision on a single beam, which would be available in real time as  
51 a diagnostic tool to the operators. Also, physics reference channels such as  
52  $e^+e^- \rightarrow \mu^+\mu^-\gamma$  where the muons are resonant with the known  $Z$ -mass are  
53 expected to provide valuable cross-checks of the collision energy scale, but  
54 only long after the data have been recorded.

55 The primary method planned to perform  $E_b$  measurements at the ILC is a  
56 non-evasive beam position monitor (BPM) based energy spectrometer similar  
57 to a setup used for calibrating the energy scale for the  $W$ -mass measurement  
58 at LEP-II [2]. At the ILC, however, the parameters of the spectrometer are  
59 tightly constrained to provide limited emittance dilution at the highest ILC  
60 energy of 500 GeV.

61 Initially, a 3-magnet chicane located upstream of the interaction point just  
62 after the energy collimators of the beam delivery system (BDS) was proposed  
63 [3]. But the baseline ILC spectrometer design uses two dipole magnets to  
64 produce a beam displacement  $x$ , while two more magnets return the beam to  
65 the nominal beam orbit. For such a chicane, the beam energy is then given  
66 by

$$E_b = \frac{c \cdot e \cdot L}{x} \int_{magnet} B dl \quad , \quad (1)$$

67 where  $L$  is the distance between the first two magnets and  $\int B dl$  the B-  
 68 field integral in each magnet. The 4-magnet chicane avoids spurious beam  
 69 displacement signals in the BPMs due to beam tilts, and thus systematic  
 70 errors in  $E_b$  measurements. For this reason, a 4-magnet spectrometer, which  
 71 maintains the beam axially with respect to the axis of the cavity BPMs, is  
 72 preferable over a more conventional 3-magnet chicane. In both cases the B-  
 73 field in the spectrometer chicane can be recorded and reversed for studying  
 74 systematic effects without changing the beam direction downstream of the  
 75 spectrometer.

76 When operating the spectrometer with a fixed dispersion of 5 mm at the  
 77 center over the whole energy range, a BPM resolution better than  $0.5 \mu\text{m}$   
 78 is needed. This resolution can be achieved with cavity BPMs [4]. Since the  
 79 spectrometer bending magnets need to operate at low fields when running the  
 80 ILC at the  $Z$ -pole, the B-field measurement may not be accurate enough to  
 81 provide the required level of precision. Significantly improved BPM resolu-  
 82 tion would however allow to run the magnets at the same field for both the  
 83  $Z$ -pole and highest energy operation.

84 An absolute energy measurement requires that the beam orbit measure-  
 85 ment is referenced to the orbit with no field applied. Unfortunately, the  
 86 residual fields still have an impact on the beam orbit at a level that may af-  
 87 fect the overall beam energy accuracy. There is an ongoing R&D program to  
 88 determine how to perform accurate field measurements for very low magnetic  
 89 fields [5].

90 Some original energy resolution studies of the SLAC prototype 4-magnet  
 91 chicane were published by M. Viti in his PhD thesis [6]. His analysis used  
 92 calibrated beam position readings but revealed that due to small differences  
 93 between the magnets in the chicane the beam inclination also needs to be  
 94 considered. It was soon realised that the same analysis could be extended  
 95 by using complex BPM readings that contain the information on both the  
 96 beam offset and inclination. This approach eliminates the need for position  
 97 calibration of the BPMs, while the whole system could be calibrated by  
 98 means of an energy scan.

99 In this publication we present the analysis based on that idea, estimate  
 100 the resolution of the spectrometer to compare it with the result of  $8.5 \cdot 10^{-4}$

101 measured in [6]. We also consider the impact of different systematics on the  
102 energy measurement in order to improve the resolution to below the  $10^{-4}$   
103 level in future experiments.

## 104 2. Test Beam Setup and Spectrometer Hardware Configuration

105 A prototype test setup for a 4-magnet chicane was commissioned in 2006  
106 (the T-474 experiment) and extended in 2007 (the T-491 experiment) in the  
107 End Station A (ESA) beamline at the SLAC National Accelerator Laboratory  
108 [7].

109 In our experiments the electron beam generated by the main Linear Ac-  
110 celerator at SLAC was transported to the ESA experimental area through  
111 the 300 m long transfer line A including bending and focussing magnets, and  
112 diagnostic instruments such as stripline and RF cavity BPMs, charge sen-  
113 sitive toroids, a synchrotron light monitor, profile screens and diodes. The  
114 SLAC linac was providing single bunches at 10 Hz and a nominal energy of  
115 28.5 GeV, a bunch charge of  $1.6 \cdot 10^{10}$  electrons, a bunch length of 500  $\mu\text{m}$   
116 and an energy spread of 0.15%, i.e. with beam properties similar to the ILC  
117 expectations at the highest energy currently available for electrons.

118 These unique beam parameters allowed to test the capabilities of the pro-  
119 posed spectrometer under realistic beam conditions. Two feedback systems  
120 were in place for the ESA beam: one for its position and one for the energy.  
121 The position feedback stabilised the beam position and angle using cavity  
122 BPMs and corrector magnets upstream the ESA area. The energy feedback  
123 stabilised the energy feeding back on the phase of the klystrons of the linac  
124 and was also used for offsetting the energy from the nominal in  $\pm 100$  MeV  
125 range.

126 The setup, as schematically shown in Fig. 1, includes four bending mag-  
127 nets denoted as 3B1, 3B2, 3B3 and 3B4, forming a chicane in the horizontal  
128 plane and high-precision cavity BPMs upstream, downstream and in between  
129 the dipole magnets. Two of which (BPMs 4 and 7) in the middle of the chi-  
130 cane were instrumented with precision movers. Horizontal positions of three  
131 monitors (BPMs 5, 4 and 7) were monitored with a Zygo interferometer [zygo  
132 ref].

133 10D37 magnets from the old SPEAR injection beamline refurbished for  
134 the use in the chicane are 37" long, 10" wide on the pole faces and have  
135 a 3" gap. They were run in series from a single power supply to minimize  
136 relative drifts. We studied the magnets during a set of measurements in

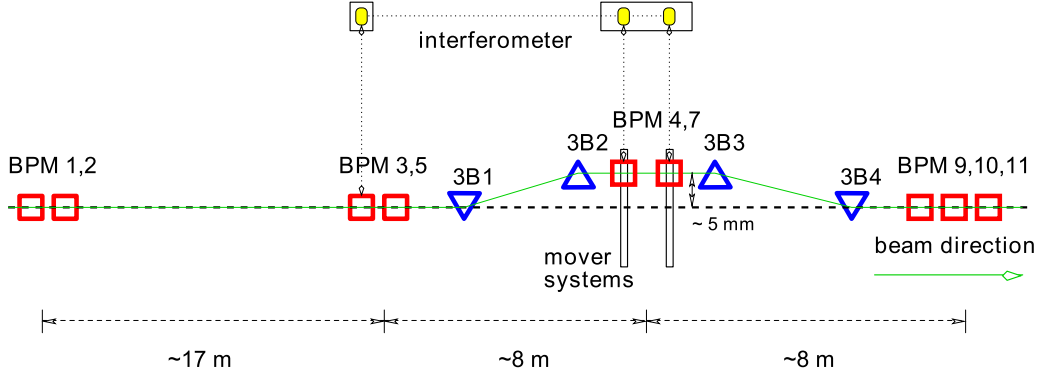


Figure 1: Schematic representation of the prototype spectrometer in ESA.

137 the SLAC’s Magnet Measurement Laboratory. Magnetic field maps of the  
 138 vertical field component  $B_y$  were taken using NMR and Hall probes, while  
 139 each  $\int B dl$  was measured using a flip coil, which was calibrated against a  
 140 moving wire system. Stability and reproducibility were at the focus of these  
 141 measurements. Details of the field measurements can be found in [8, 6, 9].

142 In situ at ESA, two NMR probes with different but overlapping working  
 143 ranges and one Hall probe were installed in the first magnet 3B1, while one  
 144 NMR probe was positioned in each other three magnets, so that field integral  
 145 values could be monitored. In the test data runs, the nominal B-field was  
 146 0.117 Tesla·m which corresponds to a magnet operation with 150 A. The  
 147 stray field outside the magnets in the middle of the chicane was monitored  
 148 using two low-field fluxgate magnetometers. One was placed on the girder to  
 149 obtain x- and y-field components and the other on the beam pipe measuring  
 150 the y-component only. Properties of the probes and the fluxgate monitors  
 151 are summarized in Tab. 1.

152 [check the probes location, discuss NMRs]

153 In order to measure the beam orbit, 8 cavity BPMs all operating in the  
 154 S-band of the RF, were installed. Three of them were SLAC prototype ILC  
 155 BPMs (3, 4, 5) using cylindrical cavities with x- and y-waveguides for the  
 156 dipole mode coupling and monopole mode suppression. Each of the five  
 157 SLAC linac type BPMs (1, 2, 9, 10, and 11) consists of three cavities: two  
 158 rectangular ones for x and y separately to avoid x-y couplings, and one  
 159 cylindrical cavity to provide charge and phase information. BPM 7 was a  
 160 dedicated ILC prototype designed and manufactured in the UK for the use

Table 1: Types of probes used for the magnetic chicane in ESA.

Name and Type of the device	Field component	Working range
NMR 3B1A		0.043 - 0.13 T
NMR 3B1B		0.09 - 0.26 T
NMR 3B2C		0.09 - 0.26 T
NMR 3B3D		0.09 - 0.26 T
NMR 3B4E		0.09 - 0.26 T
Hall probe	Y Component	
Fluxgate 1	Y/X Component	
Fluxgate 2	Y Component	

161 in the spectrometer. Unfortunately, this monitor could not be used in the  
 162 analysis due to manufacturing problems [ukbpm]. Details on the performance  
 163 of the BPM system and information on the A-line configuration can be found  
 164 in [4].

165 BPMs 12 and 24 in the A-line are placed in high-dispersion points [check  
 166 numbers] of the bending arc. In our experiment, they were instrumented  
 167 with the same high-sensitive electronics as all other BPMs in the ESA beam-  
 168 line, so that energy measurements in the A-line and in the chicane could be  
 169 performed simultaneously and cross-checked against each other.

### 170 **3. Performance of the Prototype Spectrometer**

#### 171 *3.1. Reconstruction of the beam orbit in the middle of the chicane*

172 As the chicane magnets bend the beam in the horizontal (x-) plane, we  
 173 are mainly interested in the horizontal beam position and angle, and, unless  
 174 specified otherwise, we talk about the x-coordinate throughout this section.

175 The offset of the beam trajectory in the middle of the chicane, see eq. (1),  
 176 has to be measured with respect to the nominal orbit position reconstructed  
 177 using BPMs outside of the chicane. In order to predict the readings of BPM 4  
 178 data from run 2747 were taken, with zero-current in the magnets and neither  
 179 the beam nor the hardware were manipulated. Data from a run with magnets  
 180 on could also be used for relative measurements and would result in some  
 181 better prediction, but due to the residual disperion in the beamline beam  
 182 positions before and in the middle of the chicane are correlated. For that  
 183 reason, only data from a run with magnets off were used.

184 When the magnets are on, BPMs 9, 10 and 11 were excluded from the  
 185 prediction matrix because the impact of the chicane on the beam orbit is not  
 186 fully compensated due to of the differences between the magnets.

187 Due to alignment errors, there is also a correlation between the vertical  
 188 beam position and angle before the chicane and the horizontal beam position  
 189 and angle in the mid-chicane. Therefore, both x- and y-readings from the  
 190 BPMs upstream of the chicane (x1, x2, x3, x5, y1, y2, y3 and y5) were used  
 191 in the analysis.

192 In our system signals generated by the BPMs were digitized and stored in  
 193 data files for each event, i.e. for each beam trigger. They are then digitally  
 194 converted to the baseband to decode the envelope [4]. A complex digital  
 195 local oscillator signal allows to decode both the amplitude and the phase of  
 196 the signal's phasor along the waveform. Sampled at a point close to the peak  
 197 and normalized by the phasor from the reference cavity, it gives the real,  
 198 in-phase (I), value and the imaginary, quadrature (Q), value, which contain  
 199 the information on the beam offset as well as the inclination.

200 In order to reconstruct the beam orbit in the mid-chicane, the I and Q  
 201 values from BPM 4 are correlated to the I and Q values from the upstream  
 202 BPMs we used the Singular Value Decomposition (SVD) method [10] from  
 203 several thousands of readings. Inversion of the matrix of the measured I and  
 204 Q values for the selected BPMs provides a vector of coefficients which relate  
 205 the I's and Q's of each BPM to those of BPM 4 so that a prediction can be  
 206 made:

$$I_{BPM4} = \alpha_0 + \sum_i \alpha_i^{(I)} \cdot I_i + \sum_i \alpha_i^{(Q)} \cdot Q_i \quad (2)$$

$$Q_{BPM4} = \beta_0 + \sum_i \beta_i^{(I)} \cdot I_i + \sum_i \beta_i^{(Q)} \cdot Q_i, \quad (3)$$

207 where  $\alpha$ 's and  $\beta$ 's are the SVD coefficients.

208 The difference between the predicted and the measured values is called  
 209 residual. In our case, the RMS residual is the precision of the orbit prediction  
 210 and the resolution of BPM 4 added in quadrature. It sets the limit on the  
 211 spectrometer resolution. The measured and predicted values for I and Q are  
 212 plotted against each other in fig. 2. The points in these plots lie around  
 213 the  $x = y$  bysector lines shown in solid, which means the prediction works  
 214 correctly. The histograms in the bottom part of fig. 2 show the residuals, for  
 215 both the I and Q values.

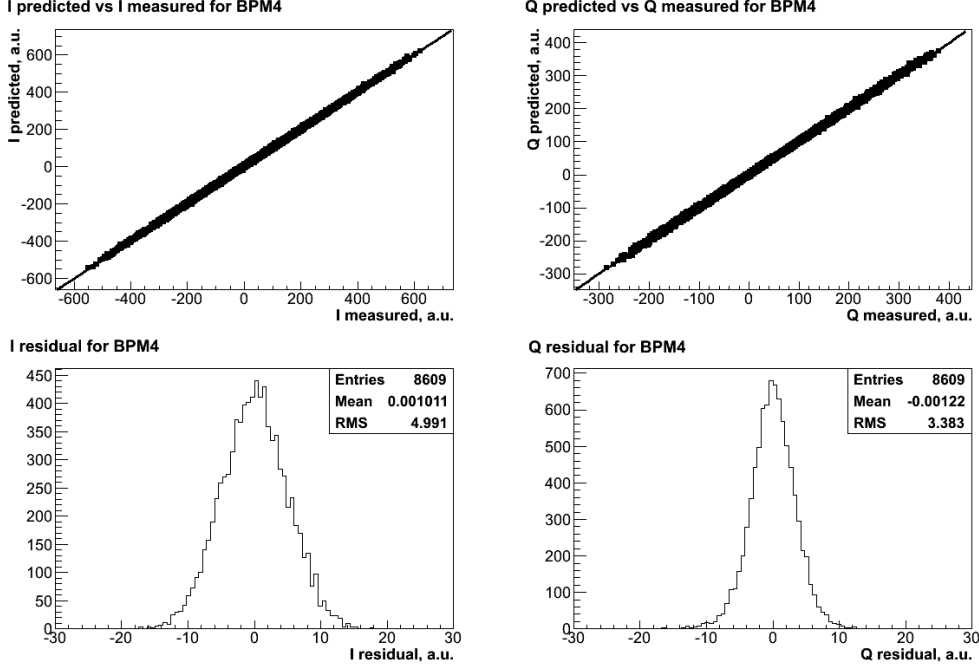


Figure 2: BPM 4 readings predicted from other BPMs in the beamline for run 2747: I predicted vs I measured (top left), Q predicted vs Q measured (top right), I prediction residual (bottom left), Q prediction residual (bottom right).

216 It is clear that the I and Q residuals for BPM 4 are small compared to  
 217 the average I and Q values, but the results in fig. 2 are still hard to interpret  
 218 quantitatively. In order to set a scale we used the mover scan data. During  
 219 the mover scan BPM 4 was moved in 0.25 mm steps from -0.5 to +0.5 mm  
 220 off the nominal position. Fig. 3 shows the scan data as well as the position  
 221 residual, which was calculated for the data used in SVD computations above.  
 222 A position residual of  $2.73 \mu\text{m}$  was estimated, which is close to the estimate  
 223 in [6], and the difference is down to the applied cuts. Taking into account a  
 224 5 mm average beam offset in the middle of the chicane for magnets on, this  
 225 sets an energy resolution limit of  $5.5 \cdot 10^{-4}$  for our spectrometer prototype.

226 Our earlier publications [4], however, revealed a  $1 \mu\text{m}$  level of resolution  
 227 of the BPM system. Due to the larger beam jitter during the energy mea-  
 228 surements the gain of the BPM electronics had to be reduced for some BPMs,  
 229 which, combined with a reduced bunch charge, decreased the sensitivity and



230 therefore a worse resolution was obtained.

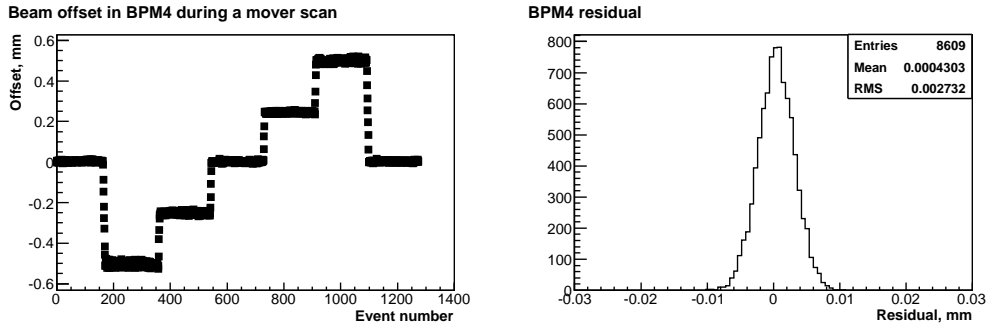


Figure 3: BPM 4 position for a horizontal mover scan (left), BPM 4 residual during a quiet period, run 2747 (right).

### 231 3.2. Dipole magnets

232 An essential prerequisite of the spectrometer is that the beam position  
233 downstream of the chicane is not energy dependant, and the upstream beam  
234 path is restored downstream. In other words, the chicane has to act on  
235 the beam in a symmetric manner. B-field measurements were performed in  
236 March 2007 to study the response of the chicane. Some results are shown  
237 in fig. 4. Here, the differences between the measured and nominal B-fields  
238 are plotted as a function of the nominal value, for negative and positive  
239 polarities.

240 In these measurements the field of the magnet 3B1 was monitored with  
241 a Hall probe, whereas for the other magnets NMR probes were used. As can  
242 be seen, 3B1, 3B2 and 3B3 follow the same trend, with a difference of a few  
243 tenths of a mT between 3B2 and 3B3, while 3B1 is off by about 1 mT. Magnet  
244 3B4 shows field values much closer to the nominal ones, because only for this  
245 magnet a more accurate relation between the current and the field (as given  
246 in [6]) was determined and used for the field settings. The differences in fig. 4  
247 can be attributed to the residual B-field, which was estimated to be  $0.2 \div 0.4$   
248 mT (see [6]), which is expected to depend on the history of the magnets  
249 and on the properties of the core material (as the design and composition of  
250 steel cores were not carefully accounted for). As a consequence, the path of  
251 the beam upstream was not fully restored downstream of the chicane, and

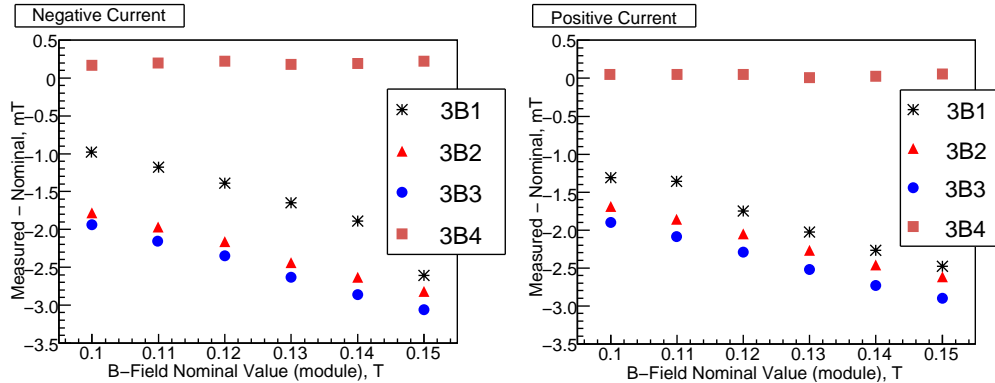


Figure 4: Differences between the measured and nominal B-fields as a function of the nominal value of the four magnets in ESA: Negative current (left); Positive current (right).

252 changes of the beam energy are converted into position variations in BPMs  
 253 9, 10 and 11.

254 Using the data from the upstream BPMs the nominal beam position in the  
 255 downstream BPMs can be predicted. Consider only BPM 9 measurements  
 256 after subtraction of the downstream BPM prediction for an energy scan we  
 257 can clearly recognize a step-like behaviour in energy, fig. 5. This observation  
 258 supports the assumption that the BPMs downstream of the chicane should  
 259 not be used to predict the nominal beam orbit in BPM 4. At the same time  
 260 we have to note that, although the net-integral field applied to the beam by  
 261 the chicane is very small, and BPM 9, which has a higher resolution than  
 262 BPM 4, is still able to resolve the energy changes during the scan.

### 263 3.3. Resolution of the energy BPMs

264 In order to estimate the resolution of the energy BPMs 12 and 24 we  
 265 plotted their Q readings versus their I readings for an energy scan. Such  
 266 a plot is shown in fig. 6 for BPM 12, left. When the energy changes, the  
 267 readings should slide up and down the line fitting the measured points, while  
 268 the noise can produce an offset from the line and move the IQ values along  
 269 the line.

270 The scale for each energy BPM was also found from the energy scan data  
 271 averaging the IQ amplitude for each step and comparing the change of the  
 272 amplitude to the energy offset given by the linac feedback. The scales and

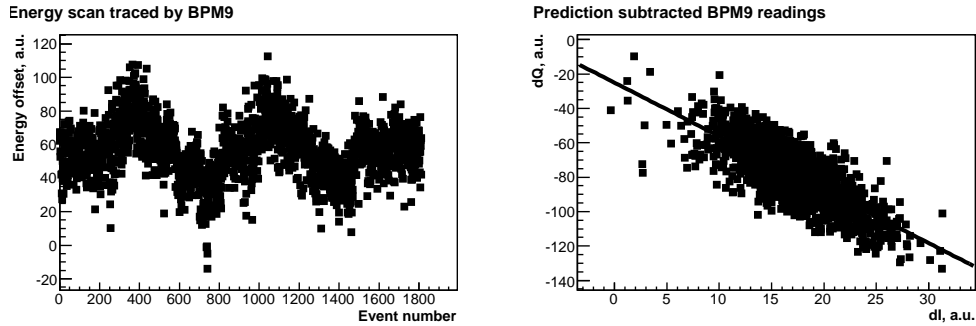


Figure 5: Energy measured by BPM 9 during the scan (left), IQ plot of the measured BPM 9 readings with the predicted readings subtracted (right). The fitted line shows the IQ rotation of the energy measurements.

273 IQ rotations allow for the energy offset to be calculated from the measured  
 274 I and Q values for both BPMs 12 and 24.

275 Measuring the average residual between the fitted line and the measured  
 276 points (fig. 6, right), we can estimate the resolution of the BPMs. As we know  
 277 the scale, the resolution can be expressed in terms of the energy. In this way  
 278 we found a 0.41 MeV resolution for BPM 12 and 2.26 MeV for BPM 24, or  
 279  $1.4 \cdot 10^{-5}$ , respectively,  $7.9 \cdot 10^{-5}$  at the nominal 28.5 GeV beam energy. The  
 280 difference can be explained by the fact that BPM 12 had an additional 20 dB  
 281 amplifier installed in its electronics chain in order to compensate for cable  
 282 losses, which reduced the effect of the noise and the granularity introduced  
 283 by the digitizers.

284 These estimates only take into account the noise in the BPM itself. It  
 285 does not take into account any other effects such as the beam jitter and the  
 286 changes of the fields in the magnets which generate the high dispersion. In  
 287 fig. 7 we compare the readings of BPMs 12 and 24 after the energy calibration.  
 288 An RMS residual of 5.5 MeV ( $1.9 \cdot 10^{-4}$ ) was found, which is about two times  
 289 bigger than the noise measurements of 2.3 MeV from above if combined in  
 290 quadrature. This indicates that the resolution of the energy measurements  
 291 of BPMs 12 and 24 is not limited by the BPM noise alone, but still allows  
 292 to measure small fluctuations of the energy and provides a reference energy  
 293 value to better than  $1.9 \cdot 10^{-4}$ .

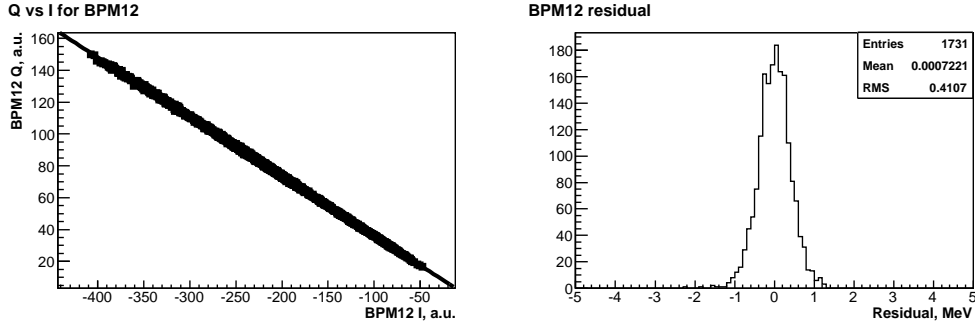


Figure 6: Resolution estimation for BPM 12: Q vs I for the energy scan (left), residual between the measured values and the IQ line in terms of energy, multiplied by the scale (right).

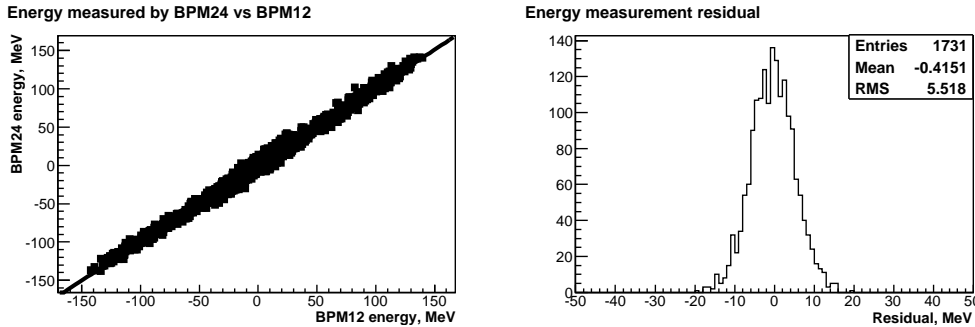


Figure 7: Comparison of BPMs 12 and 24: BPM 24 energy measurement vs BPM 12 (left), residual between BPM 12 and 24 measurements (right).

### 294 3.4. Energy resolution of the spectrometer

295 The readings predicted for BPM 4 by all other BPMs can be subtracted  
 296 from the measured values and, when the magnets are on, provide energy  
 297 measurements as the position and angle change in the mid-chicane (fig. 8).  
 298 The energy, in turn, can be predicted from the energy BPMs 12 and 24. The  
 299 residual, besides the resolutions of each BPM, depends on the fluctuations  
 300 of the magnetic fields, mechanical vibrations, as well as drifts and other  
 301 systematic effects and non-linearities.

302 We first compare the relative energy measured by BPM 4 with the mea-  
 303 surements of BPM 12 (fig. 8, top). This results to a resolution of 27.3 MeV  
 304 or  $9.6 \cdot 10^{-4}$ . As this is much higher than the precision of the orbit reconstruc-

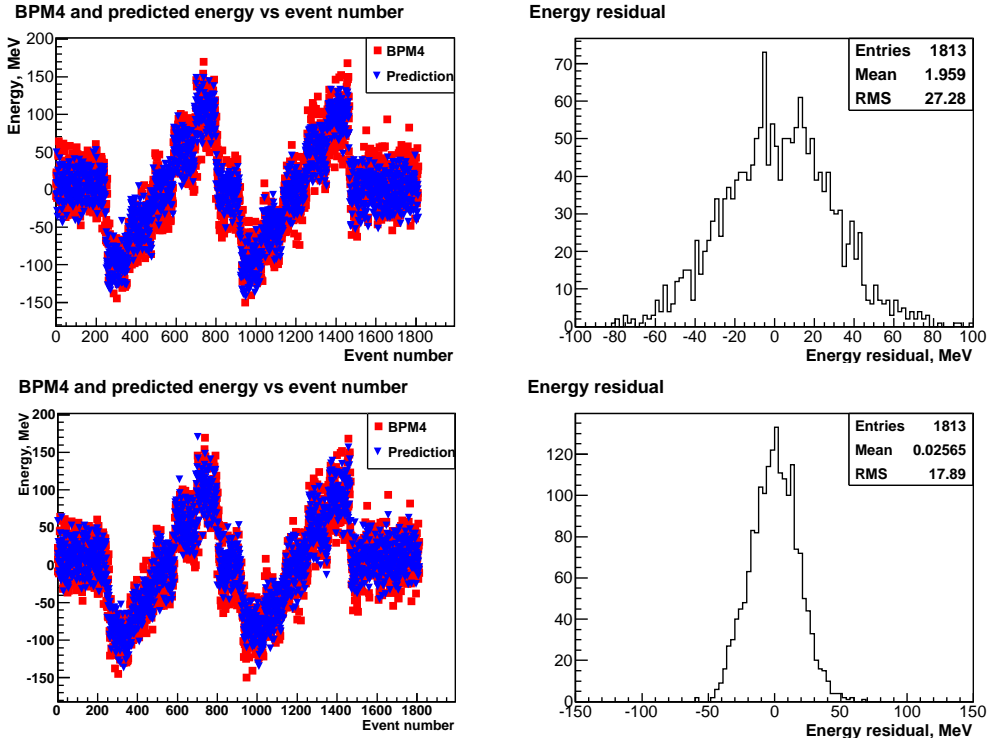


Figure 8: Energy resolution measurement: energy measured by BPM 12 and BPM 4 (top left), residual between BPM 12 and BPM 4 readings (top right), energy measurement predicted by BPMs 12, 24 and additional parameters and BPM 4 reading (bottom left), residual between the prediction and BPM 4 reading (bottom right).

305 tion, we decided to look for correlations using additional data and applying  
 306 the SVD method by starting again from BPM 12 (but this time the scale is  
 307 corrected by SVD to better match BPM 4 readings which results to a lower  
 308 residual) and then adding more data in the matrix to better reconstruct the  
 309 spectrometer measurements and understand the systematics. Table 2 sum-  
 310 marises the results. together with the residuals calculated using the same  
 311 coefficients for a quiet period when the magnets were on and nothing was  
 312 changed in the system. Looking for consistent improvements of the residual,  
 313 we can identify the main sources of systematic errors.

314 The biggest step in residual reduction is observed when the data from  
 315 BPMs 9, 10 and 11 was included in the computation. As we know, BPMs  
 316 9, 10 and 11 are sensitive to the energy, but also to the net-magnetic field

317 of the chicane. Since our system did not provide bunch-to-bunch B-field  
318 measurements, only interpolated field data could be used. If such data were  
319 involved in the analysis we did not recognize a consistent improvement. It  
320 is therefore very likely that field changes are encoded in the downstream BPM  
321 data, which might be the reason for residual improvements if these data are  
322 accounted for in the analysis.

323 Some further improvement is also noted when the charge  $Q$  is included in  
324 the analysis, even though all the BPM data were normalised by the charge.  
325 This is best explained by the fact that BPMs 12 and 24, although very  
326 sensitive to energy changes, were not centered to their operating ranges, and  
327 could be running close to saturation.

328 Ultimately, in order to achieve an energy resolution approaching  $10^{-5}$ ,  
329 one has to monitor the relative motion of the BPMs in the beamline. An  
330 interferometer, once well tuned, seems to be a reliable, fast and precision  
331 tool. But since the mechanical vibrations observed were in the region of a  
332 few hundred nanometers, the Zygo interferometer in our setup only provided  
333 a moderate improvement to the energy measurement.

334 The final result of these investigations is shown in the bottom part of  
335 fig. 8. With additional data included, the prediction tracks the spectrometer  
336 measurement a bit better than given in the plot above. The resolution was  
337 measures to 17.9 MeV (or  $6.3 \cdot 10^{-4}$ ) for an energy scan and 16.7 MeV (or  
338  $5.9 \cdot 10^{-4}$ ) for a quiet period. These numbers are very close to the estimate  
339 for the precision of the orbit reconstruction of  $5.5 \cdot 10^{-4}$ , which means that  
340 the weighting of different systematics has been performed correctly.

### 341 *3.5. X to Y coupling*

342 Even though the spectrometer chicane operates in the horizontal plane,  
343 the energy scan is also traced in the vertical plane. Firstly, because of the  
344 alignment errors the beam receives a small bend in the vertical direction.  
345 Secondly, there is an internal cross-talk between the x and y couplers of the  
346 BPM, a virtual offset in y is created by an offset in x.

347 In order to estimate the total cross-coupling between the x and y planes  
348 of the spectrometer we, again, considered the energy scan data (run 2743),  
349 but this time predicting the vertical beam position in BPM 4 using SVD  
350 coefficients obtained from data in run 2747. Clearly, the energy scan is  
351 traced in the measured y-offset (fig. 9, left). We had to take into account  
352 that the sensitivity of the x and y channels of BPM 4 was different, so we  
353 used mover scan data for both to get the position scale, which we then used

Table 2: Energy residuals calculated for BPM 4 including additional parameters.

Data included	Residual, MeV		$\Delta E_b/E_b$ contribution, $\times 10^{-4}$	
	energy scan	quiet period	energy scan	quiet period
BPM 12	26.83	24.63	–	–
BPMs 12, 24	26.41	24.76	1.7	+0.9
BPMs 12, 24 and B-field	25.94	25.88	1.7	+2.6
BPMs 12, 24, charge and B-field	23.48	22.52	3.9	4.5
BPMs 12, 24, 9, 10, 11, B-field and charge	18.15	17.47	5.2	5.0
BPMs 12, 24, 9, 10, 11, B, q and interferometer	17.89	16.71	1.1	1.8
BPMs 12, 24, 9, 10, 11, B, q, interferometer and fluxgate	17.89	16.71	–	–

354 to normalise the raw energy. For that reason the energy is in units of mm in  
 355 fig. 9, although one should keep in mind that an energy change causes both  
 356 the offset and the incline to change in the middle of the chicane.

357 The plot in fig. 9, right, shows the correlation between the energy mea-  
 358 sured in both planes. From the incline of the line fitting the data in this plot  
 359 we calculated a rotation of almost  $25^\circ$ , or an x-y isolation of about 7.6 dB.  
 360 The rotation is too large to be attributed entirely to the alignment, at the  
 361 same time the x-y isolation is too poor to be caused by the BPM (usually  
 362 providing about 20 dB isolation without tuning), which indicates that both  
 363 effects take place. It is therefore important to minimize the x-y cross-talk  
 364 in the BPMs and eliminate fake offsets, and carefully align the elements  
 365 of the spectrometer to avoid negative effects on the beam and the energy  
 366 measurement.

### 367 3.6. Estimate of the absolute beam energy

368 So far we have been talking about the relative energy measurement, i.e. a  
 369 measurement of the energy offset from some nominal value, which we assumed  
 370 to be 28.5 GeV, the beam energy we requested for our ESA runs. Below we

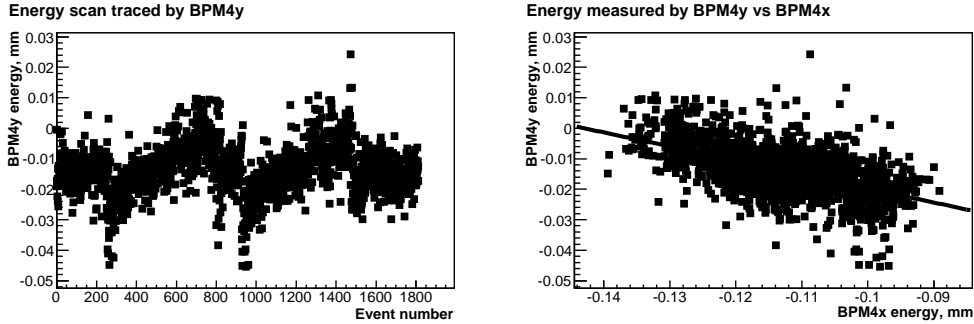


Figure 9: Effect of the chicane on the vertical beam trajectory: energy scan traced by BPM 4 in y (left), energy data measured by BPM 4 in y vs x (right), position calibration was used in order to exclude the difference in sensitivities, hence, the energy is calibrated in units of the offset (mm).

371 estimate the beam energy using the values we obtained in the previous steps  
 372 of the analysis, such as the energy and position scales.

373 When the magnets are turned on, BPM 4 is moved by a few mm in order  
 374 to return the beam offset into its dynamic range. This move is observed by the  
 375 precision Zygo interferometer. From prediction subtracted BPM 4 readings  
 376 we found IQ rotations and scales for the position and energy changes.

377 According to the interferometer, BPM 4 was moved by 4.035 mm between  
 378 runs 2743 (magnets on) and run 2747 (magnets off). Using the IQ rotation  
 379 and scale we obtained from the mover scan we can predict the changes of the  
 380 I and Q values of BPM 4 an offset of 4.035 mm would create, even though  
 381 in reality large offsets saturate the electronics. Our calculations resulted  
 382 in  $I = 7078.6359$  and  $Q = 3702.9554$ , which we added to the prediction  
 383 subtracted I and Q values obtained from the energy scan (fig. 10, right). In  
 384 this process we rotate the IQ plane for the energy scan data, so we have to  
 385 find the new value of the IQ rotation for the energy line, but the energy scale  
 386 still applies. Using this scale and the new IQ rotation for the energy, we can  
 387 now calculate the absolute energy (fig. 10, left). This calculation resulted in  
 388 a measured nominal energy of 26.37 GeV.

389 Our estimate is over 2 GeV, or more than 7%, off the nominal value. The  
 390 linac was likely to run at a lower energy at the time of the experiment as some  
 391 of the klystrons were offline, but 26.37 GeV seems to be too low an energy.  
 392 At the same time, looking back at our analysis, fig. 10 right, we notice  
 393 that the absolute measurement is very sensitive to the BPM resolution: a



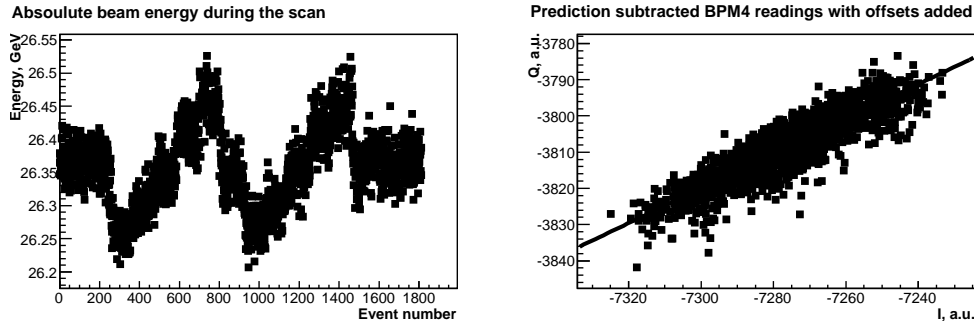


Figure 10: Reconstruction the absolute beam energy: a scan around the nominal energy(left), IQ plot for BPM 4 offset in both I and Q to take into account the BPM was moved horizontally by 4.035 mm (right).

394 small change of the energy line rotation applied to large I and Q values can  
 395 significantly change the result. The same argument applies to the position  
 396 IQ rotation and scales – small errors are exaggerated when combined and  
 397 multiplied by large numbers.

398 Clearly, any improvement of the BPM resolution would have a positive  
 399 impact on the absolute energy measurement, but simplifying the procedure  
 400 itself, which means fitting the beam offset into the dynamic range of the  
 401 BPMs, may be even more efficient as it eliminates the need for position  
 402 calibration and excludes the associated systematics.

403 [Can we get the energy from somewhere else for comparison???

#### 404 4. Suggestions for the future experiments

- 405 improve BPM resolution
- 406 provide B-field measurements at the beam repetition frequency
- 407 make sure the beam is centered
- 408 3-magnet chicane (doublet-magnet-triplet-spectrometerMagnet-triplet-magnet-
- 409 doublet) – but think about the residual dispersion, offset BPMs with magnets
- 410 off to use the full range
- 411 Zygo for the triplets

412 **5. Summary**

413 **References**

- 414 [1] J. Brau, (ed. ), et al., International Linear Collider reference design  
415 report. 1: Executive summary. 2: Physics at the ILC. 3: Accelerator. 4:  
416 Detectors ILC-REPORT-2007-001.
- 417 [2] R. Assmann, et al., Calibration of centre-of-mass energies at LEP2 for  
418 a precise measurement of the W boson mass, Eur. Phys. J. C39 (2005)  
419 253–292. arXiv:hep-ex/0410026.
- 420 [3] V. N. Duginov, et al., The beam energy spectrometer at the Interna-  
421 tional Linear Collider, DESY LC Notes, LC-DET-2004-031.
- 422 [4] M. Slater, et al., Cavity BPM system tests for the ILC en-  
423 ergy spectrometer, Nucl. Instrum. Meth. A592 (2008) 201–217.  
424 doi:10.1016/j.nima.2008.04.033.
- 425 [5] N. Morozov, Progress report on developments of the magnetic field  
426 measurements techniques (21-23 May and 21-23 November 2005).  
427 URL [http://zms.desy.de/aktuelles/veranstaltungen\\_in\\_zeuthen/  
428 konferenzen/2005/index\\_ger.html](http://zms.desy.de/aktuelles/veranstaltungen_in_zeuthen/konferenzen/2005/index_ger.html)
- 429 [6] M. Viti, Precise and Fast Beam Energy Measurement at the Interna-  
430 tional Linear Collider, Ph.D. thesis, dESY-THESIS-2010-007 (2010).
- 431 [7] M. Hildreth, et al., Linear Collider - BPM-based energy spectrometer  
432 (2004).  
433 URL [http://www-project.slac.stanford.edu/ilc/testfac/ESA/  
434 projects/T-474.html](http://www-project.slac.stanford.edu/ilc/testfac/ESA/projects/T-474.html)
- 435 [8] H. Schreiber, et al., Magnetic Measurements and Simulations of a 4  
436 Magnet Dipole Chicane for the International Linear Collider Particle Ac-  
437 celerator Conference PAC07 25-29 Jun 2007, Albuquerque, New Mexico.
- 438 [9] S. Kostromin, M. Viti, Magnetic Measurements for Magnets 10D37,  
439 iLC-SLACESA TN-2008-1 (2008).  
440 URL [http://www-project.slac.stanford.edu/ilc/testfac/ESA/  
441 TechNotes/TN-2008-1.pdf](http://www-project.slac.stanford.edu/ilc/testfac/ESA/TechNotes/TN-2008-1.pdf)
- 442 [10] W. H. Press, et al., Numerical Recipes in C, Cambridge University  
443 Press, 1992.